Lightweight reinforcement systems for fatigue cracked orthotropic bridge decks

Abstract

Two systems for reinforcing “in-service” orthotropic bridge decks (OBDs) have been researched: the bonded steel plates system and the sandwich steel plates system. The main idea of these type of reinforcements is to stiffen the existing deck plate, thereby reducing the stresses at the fatigue sensitive details, and thus extending the fatigue life of the OBD. Both reinforcement systems consist of adding a second steel plate to the existing steel deck. The behaviour and the effect of the reinforcement systems on full-scale OBD are investigated. Full-scale static tests and finite element analyses were performed on reinforced deck panels, using realistic wheel loads. The results showed at least 40% of stress reduction close to the fatigue sensitive details after applying both reinforcements. The two suggested reinforcement systems showed a good performance and proved to be efficient lightweight solutions to refurbish orthotropic bridge decks and extend their life span.

Keywords: orthotropic decks, bridges, reinforcement, refurbishment, sandwich structures, adhesive bonding.

1. Introduction

Orthotropic bridge decks are extremely cost-effective solutions when low dead-weight is an important factor. For this reason they are largely used in most of the major long span bridges in the world and in movable bridges [1,2]. Figure 1 shows a typical cross section of an OBD which consists of a deck plate supported in two mutually perpendicular directions by a system of longitudinal stiffeners (usually of trapezoidal shape) and transverse crossbeams. The whole deck is supported by main girders. All these elements are connected by welding.

Fatigue is a well-known phenomenon in orthotropic bridge decks. Some welded details turn out to be extremely sensitive to fatigue loading and shorten the expected life span of OBDs. The fatigue sensitivity is dependent on the geometric details of the welded joints, on the elements slenderness adopted and on the traffic volume of heavy vehicles. Numerous examples of fatigue cracks found at several welds have been reported in Europe [3], in Japan[4] in China[5] and in Brazil[6].

One of the most threatening fatigue cracks is the one at the longitudinal welds between the deck plate and trapezoidal stiffener (deck-plate-to-stiffener weld)[7-9]. The crack is only detected at a late stage, when it has already grown through the complete deck plate thickness. The crack initiation point is of very difficult access which delays visual detection. As the crack grows through the deck plate thickness, it largely endangers the traffic safety running on the bridge. Moreover, these fatigue cracks have been detected in an unexpected early age of OBD. A known case-study is the 12 mm thick orthotropic steel deck plate of the heavy loaded bascule bridge of the Van Brienenoord Bridge in the Netherlands[3,7]. These types of cracks at the crossbeam location were detected after only seven years of the bridge service-life[3].

One of the main reasons for the short fatigue life of these welds is the low stiffness of the deck plate, which is insufficient to deal with the wheel loads of heavy traffic[7,10]. Therefore, it became clear that renovation techniques were needed to stiffen the existing deck plate, thereby reducing the stresses at the fatigue sensitive details, and extending the fatigue life of the OBD. Design norms have been revised to avoid these fatigue problems in newly design OBD.

Research projects have studied different renovation systems to strengthen existing orthotropic steel bridge decks[7, 10-14]. The main idea is to add a stiff layer on the top of the existing deck to increase its total stiffness. Up to now, most of the studies were focused on reinforcement techniques for fixed bridges. The most popular solution is to replace the classic asphalt layer by a concrete overlay[7, 13-14]. However, OBDs are also widely used in movable bridges. In this case, the reinforcement's dead-weight is a major parameter when choosing the most efficient solution. It is therefore important to find more efficient lightweight solutions to reinforce movable orthotropic bridges.

The research presented in this paper is focused on two lightweight solutions for strengthening a movable OBD: the bonded steel plates system and the sandwich steel plate system. Both systems consist of adding a second steel plate to the existing steel deck. In the bonded steel plates system, the second steel plate is bonded to the existing deck by vacuum infusing a 2 mm thick adhesive layer between the two steel plates (the existing deck plate and the second steel plate). Preliminary research conducted on this bonding system showed promising results[7, 15]. In the sandwich steel plate system, the existing deck is reinforced by adding a sandwich overlay, consisting of a 15 to 30 mm thick polyurethane core and the second steel plate. The sandwich system has been initially developed to repair and upgrade ferry decks, but has been applied in many other fields including new bridge decks and repair of existing decks[16-18]. Both techniques can be considered lightweight solutions to refurbish OBDs (between 50 and 80 kg/m^2).

The first part of the research was focused on the characterization of the flexural behaviour of the two reinforcements. Bending static and fatigue tests were performed on reinforced beams. The effect of temperature, geometry and load conditions on the stiffness and fatigue life of the reinforcements systems has been studied[19-21]. Secondly, a real application of the bonded system was monitored on a pilot application to reinforce a movable OBD in the Netherlands[22]. Strain data recorded before and after the bridge reinforcement show significant stress reduction in the fatigue sensitive details.

In this paper, the third part of the research is presented. The research is focused on the full scale behaviour of reinforced deck panels. The effect of the bonded and sandwich steel plates reinforcement systems is investigated by conducting full-scale laboratory tests and numerical simulations on reinforced deck panels. The main goal is to determine the stress reduction at the fatigue sensitive welds when the reinforced deck panels are loaded by realistic wheel prints.

2. Bridge deck specimens

2.1 Geometry

Figure 2 shows the geometry of the orthotropic deck panels built to perform the full-scale tests. Two independent deck panels were reinforced, one using the bonded steel plates system – Specimen 1, and the second one using the sandwich steel plates system – Specimen 2. The two decks had exactly the same geometry. The deck panels are 5000 mm long and 2000 mm wide. The deck plate is 12 mm thick and it is supported in the longitudinal direction by three trapezoidal stiffeners (troughs), so called Krupp profile FKH 2/325/6 (height of 325mm, base distance between the outer side of the trough legs of 300 mm, bottom width of 105mm and a plate thickness of 6mm), and in the transverse direction by two crossbeams 3000 mm apart (inverted T-profile: 10 mm thick by 788 high web and 200 mm wide by 16 mm thick flange) . In the actual situation, the traffic is running in the longitudinal direction on top of the deck plate. The orthotropic deck is made of steel grade S355 ($f_y = 355$ MPa, $f_u = 510$ MPa, E = 210 GPa, $\upsilon = 0{,}3$)[23].

2.2 Reinforcement

In the bonded steel plates system, the 12 mm thick deck plate was reinforced with a 6 mm thick second steel plate and a 2 mm thick adhesive layer (nominal thickness). In the sandwich steel plates, the 12 mm thick deck plate was reinforced with a 5 mm thick second steel plate and a 15 mm thick polyurethane core – see Figure 3.

In both systems, the second steel plate is made of steel grade S355. The adhesive material used for the bonded system is a low viscosity epoxy resin - Epikote resin EPR 04908 with hardener Epikure curing agent EPH 04908. The core material used for the sandwich system is polyurethane (solid polymer) with density 1150 kg/m^3. Table 1 summarizes the mechanical properties at room temperature obtained from tensile material tests performed in previous research – tensile Young's modulus E_t, tensile strength σ_{tmax} and tensile failure strain ε_{tmax} [19, 20].

Table 1: Tensile mechanical properties of the epoxy-adhesive and polyurethane-core.

Material	E_t (MPa)	σ_{tmax} (MPa)	ε_{tmax} (%)	υ (-)
Epoxy	2929	69,3	4,9	0,4
Polyurethane	721	25,0	26,6	0,36

The application of the bonded steel plates reinforcement system consisted of the following steps: (1) grit blast and clean the steel surfaces to be free from rust, grease and dust (cleaning grade Sa 2 1/2 according with ISO 8501[24]); (2) primer application on the cleaned steel surfaces; (3) glue steel spacers on the top of the existing deck plate with thickness of 2 mm; (4) place the second steel plate carefully on the top of the existing deck plate; (5) prepare the cavity between the steel plates to create vacuum; (6) vacuum inject the adhesive into the cavity; (7) cure during 16 hours between 40˚C and 50˚C.

The application procedure of the sandwich reinforcement system consisted of the following steps: (1) grit blast and clean the steel surfaces to be free from rust, grease and dust (Sa 2 1/2 [24]); (2) weld steel bars with the core thickness on the perimeter of the existing deck plate; (3) glue PU spacers with the core thickness on the existing deck plate; (4) place the second steel plate on the top of the perimeter bars and weld through the perimeter forming a cavity; (5) inject the liquid polyurethane into the cavity between the steel plates (5) cure at room temperature during 48 h.

2.3 Instrumentation

Strain gauges were applied to the existing steel deck plates, at three different cross-sections of the panels: crossbeam A, crossbeam B and midspan between both crossbeams (see Figure 2). Figure 4 shows the strain gauges applied at the midspan and at the crossbeam cross-sections.

These sections represent the two typical cross-sections where cracks at the deck-plate-to-stiffener welds are mostly detected and therefore they were selected to conduct the current study. The instrumentation plan was exactly the same for both reinforced deck specimens: sandwich steel plates system and bonded steel plates system.

All strain gauges measured transverse strains except numbers 26, 27 and 28 at the bottom of the stiffeners at the midspan cross-section, which measure longitudinal strains (Figure 4 (a)). Figure 5 shows the position of the strain gauges close to the deck-plate-to-stiffener welds at midspan between crossbeams.

3. Experimental procedure

Static tests were performed at the crossbeam sections and midspan between crossbeams. The specimens were loaded with wheel prints type B and type C in accordance with the fatigue load models of EN 1991-2[25]. Wheel print type C is a single-tyre 320 mm long and 270 mm wide, usually called super-single. Wheel print type B is a double-tyre with two single-tyres 320 mm long and 220 mm wide, that are 320 mm apart from each other.

At the crossbeam, static tests were performed at each trough-to-crossbeam joint using one wheel type C aligned with the trough. The six trough-to-crossbeam joints in each deck specimen were tested one by one. Figure 6 shows one example of a static test performed at the crossbeam A, using wheel type C aligned with the middle trough.

At midspan between crossbeams, two static tests were performed, one using wheel type C aligned with the middle trough and a second one using wheel type B (double-tyre), with one of the tyres aligned with the middle trough. Figure 7 shows the static test performed using wheel type B.

On specimen 1, tests were conducted before and after being reinforced. The static tests on the unreinforced deck are the reference tests. Specimen 2 was tested after being reinforced with the sandwich steel plates. The maximum wheel load on the static tests was 50 kN for the unreinforced deck and 100 kN for the reinforced decks. The load level was lower at the unreinforced deck in order to prevent any damage before applying the reinforcement.

The deck specimens were clamped to the ground at the bottom flange of the two crossbeams. The load was applied by a steel frame which held the hydraulic jack. A photo of the test set-up is given in Figure 8.

Two similar test-rigs were used, one for the bonded deck specimen and another for the sandwich deck specimen. The tests were load controlled and the testing speed was 0.3 kN/s. The load was applied on the deck by the following sequence: hydraulic jack, load cell, a rectangular-shaped steel plate 30 mm thick and three layers of 10 mm thick rubber with the same rectangular shape. The rectangular area was the size of the wheel prints.

4. Numerical simulation

Finite element analysis (FEA) were performed in order to simulate the structural behaviour of the reinforced OBDs when subjected to wheel loads. The main goal was to determine the stress distribution in the OBD during the static tests. Therefore the geometry, wheel loads and boundary conditions simulated as much as possible the full-scale test set-up presented previously. The simulations were performed using the commercial FEA program ABAQUS[26].

4.1 Geometry

The model's geometry is exactly the same as the bridge deck specimens presented in Figure 2. The nominal geometry of the several parts of the OBD were used in the model, namely, deck plate, second steel plate and interface layer thicknesses. The welds were not specifically modeled. They were simulated with the geometrical connection between the different elements (deck plate, stiffeners and crossbeams).

4.2 Materials

All materials were modelled as linear elastic using the mechanical properties described earlier for the steel ($E = 210$ GPa, $\upsilon = 0{,}3$), for the epoxy ($E = 2929$ MPa, $\upsilon = 0{,}4$) and for the polyurethane ($E = 721$ MPa, $\upsilon = 0{,}36$).

4.3 Loads and Boundary conditions

The loads and boundary conditions were defined in order to simulate as close as possible the full-scale static tests. The two crossbeams' bottom flanges were fully clamped. A symmetry simplification was applied to the global model and therefore only half of the deck panel was simulated applying the corresponding boundary conditions. Figure 9 shows an overview of the three-dimensional finite element model (FE model). The symmetry simplification saves enormous computational time and memory. This allows to implement a more refined mesh close to the critical areas of the FE model, such as loading areas and high stress gradient areas, which leads to more accurate results.

4.4 Mesh and element type

The FE model was built using three-dimensional elements. All the parts of the structure, crossbeams, troughs, deck plate and reinforcement were modelled using continuum 20-nodes brick (solid) elements, quadratic (second-order) with reduced integration. These elements are available in the ABAQUS library as C3D20R (Continuum 3-Dimensional 20-nodes Reduced integration elements). Quadratic elements were used in order to avoid problems of shear locking. Shear locking affects the performance of linear elements subjected to bending loads[26].

Two models were built according to the load location. One model simulates OBD loaded by wheel prints at the crossbeam location (Crossbeam-FE model) and the second model simulates OBD loaded by wheel prints at midspan between crossbeams (Midspan-FE model). In each of these models, the three deck states were modelled: unreinforced, bonded steel plates reinforced and sandwich steel plates reinforced. Therefore six models were built in total.

An example of the mesh used in the analysis is shown in Figure 10. The meshes were refined close to the loading areas and where high stress levels were expected, such as close to the crossbeams and at the deck-plate-to-stiffener weld. Coarser meshes were used where the stress level were low or irrelevant for the analysis. The maximum aspect ratio of an element is 5, in order to avoid artificial stiffening, except in the areas of coarser meshes where the stress level is low and far from the loading area. Figure 11 shows the mesh details along the thickness of the unreinforced and reinforced deck plates. The FE models have between 720 000 and 1 000 000 nodes and between 150 000 and 215 000 elements. A mesh convergency study was performed to prove the mesh independency of the results[27].

5. Experimental results and numerical validation

The experimental results are presented as the strains recorded by the strain gauges at the maximum static load. These experimental values are compared with the corresponding strain distribution obtained from the FEA.

Figure 12 show the results of the bonded and sandwich reinforced deck panels. The total wheel load is 100 kN using wheel print type C. The load is applied at the crossbeam aligned with the middle trough. The graphs show the transverse strain distribution at the bottom side of the steel deck plate ε_{xx} along the width of the deck specimens, at the crossbeam cross section (CB) and 75 mm from the crossbeam cross section (75 mm CB). The experimental values (Exp.) were recorded during testing by the strain gauges applied to the deck specimens. The strain distribution is given by the FEA.

The strains measured by the gauges at the crossbeam cross section close to the loaded deck-plate-to-stiffener welds are very high, approximately -450μ in the bonded system (Figure 12a – CB Exp.) and -600 μ in the sandwich system (Figure 12b - CB Exp.). The peak stresses given by the FEA occur at the weld root. The stress concentration is extremely high close to these welds. The high stress concentration is caused by the singularity of the crossbeam web. This stress concentration is the main cause for the extremely short fatigue life of the welds at this location. The stresses are significantly lower between stiffener webs (x=1000 mm) than close to the welds. The strain values close to the welds at the cross section 75 mm from the crossbeam decrease almost 50% when compared to the crossbeam cross section (Figure 12a and 12b – 75 mm CB). Wheel loads at the crossbeam location cause mainly stresses on the loaded area (middle trough). Immediately outside the loaded area, the stresses are almost zero. In general, the numerical prediction from the crossbeam FE-models corresponds well to the experimental values.

Figure 13 and 14 show the corresponding results for the bonded and sandwich reinforced deck loaded at midspan between crossbeams by wheel type C and wheel type B, respectively. The total wheel load for both cases is 100 kN.

On both reinforcement systems, the strains recorded by the gauges close to the deck-plate-to-stiffener welds are significantly lower than at the crossbeam location (50% to 65% lower). Moreover, the strain gradient close to the welds is also lower than at the crossbeams. The strains close to the welds are slightly higher for wheel type B than for wheel type C. However the strain values between stiffeners' webs are lower for wheel type B than for wheel type C. In general, the numerical prediction from the midspan FE-model corresponds well to the experimental values.

6. Discussion

Since the FEA proved to render accurate simulations of the actual full-scale behaviour of the deck panels, the numerical results were used for further analysis. Figure 15 compares the transverse strain distribution at the bottom side of the deck plate between the unreinforced deck, bonded steel plates reinforced deck and sandwich steel plates reinforced deck. The wheel load is 100 kN and the wheel print is type C.

Results show that the transverse strains decrease significantly after applying the reinforcement systems. The strains decrease both at the crossbeam and at midspan between crossbeams. Figure 15 (a) shows that, the strains at the crossbeam location close to the deck-plate-to-stiffener welds and between the stiffener webs (x=1000 mm) are higher for the sandwich steel plates reinforcement than for the bonded steel plates reinforcement. At midspan between crossbeams (Figure 15b), the strains close to the deck-plate-to-stiffener welds are slightly higher for the sandwich reinforcement than for the bonded reinforcement. On the contrary, the strain between stiffeners' webs are lower for the sandwich than for the bonded reinforcement.

The fact that the sandwich reinforcement perform less well close to the welds is related with the high shear forces present at this deck location. According to Teixeira de Freitas et al.[28], sandwich beams decrease their bending performance when shear increases its role on the bending behaviour of the beam. This is why the sandwich steel plates have better results at midspan between crossbeam than at the crossbeam, and better results between stiffener webs than close to the welds. The bending performance of the sandwich reinforcement is much better if bending moments play a more important role than shear forces on the behaviour of the reinforced deck.

6.1 Strain reduction factor

In order to quantify the decrease of strain values at the deck after applying the reinforcements, a strain reduction factor SRF was determined for each strain gauge applied to the deck by equation (1).

$$SRF = 1 - \frac{\varepsilon_{\text{Reinforced deck}}}{\varepsilon_{\text{Unreinforced deck}}} \qquad (1)$$

The results from the strain gauges were gathered in four groups of deck locations. Figure 16 shows a drawing where the four details are defined.

Table 2 shows the average and the standard deviation values of the strain reduction factors on each group of strain gauges at the crossbeam location and at midspan between crossbeams for the bonded steel plates and the sandwich steel plates reinforcement.

Table 2: Strain Reduction Factor - SRF (average ± standard deviation).

SRF (%)	Bonded steel plates		Sandwich steel plates	
	Crossbeam	Midspan	Crossbeam	Midspan
I	56±5	48±3	47±7	45±9
II	45±3	61±3	37±8	56±3
III	62±4	81±12	48±7	48±14
IV	–[1]	23±1	–[1]	36±4

[1] There is no strain gauges of Group IV at the crossbeam cross-section (see Figure 4).

The bonded steel plates reinforcement reduces the transverse strains at the crossbeam close to the deck-plate-to-stiffener welds (groups II and III) by approximately 45% to 60%. At midspan, the reduction is higher than at the crossbeam (between 60% and 80%). The standard deviation is higher at midspan for group III because at this location two load cases are considered for determining the *SRF*, wheel type C and wheel type B. Group IV has the lowest strain reduction factor, approximately 20%. These results indicate that the reinforcement has more influence on the local strains (transverse strains, groups I, II and III) than on the longitudinal strains (group IV). The bonded steel plates reinforcement has little influence on the global behaviour of the bridge deck (longitudinal strains, group IV)

The sandwich steel plates reinforcement reduces the transverse strains at the existing deck plate by approximately 40% to 55% (groups I, II and III). The differences between *SRFs* at midspan between crossbeams and at the crossbeam are not as significant as for the bonded steel plates reinforcement, except for group II. The longitudinal strains at the bottom of the stiffener are reduced by about 35% (group IV). This value is higher than for the bonded steel plates. The sandwich steel plates reinforcement influences the local behaviour (transverse strains: I, II, III) as well as the global behaviour of the deck (longitudinal strains: IV).

The sandwich steel plates can be considered as a global reinforcement system while the bonded steel plates as a local reinforcement system.

The aim of the reinforcement systems is to extend the fatigue life of the OBD. This fatigue life is limited by the fatigue cracks that grow at the deck-plate-to-stiffener welds. Therefore the most important *SRFs* for the fatigue life of the bridge are from group II and group III, which represent gauges measuring strains close to these welds. These strains decrease at least 45% and 37% at the crossbeam location after applying the bonded and sandwich reinforcement systems, respectively (minimum values of group II and III at the crossbeam). At midspan between crossbeams, these strain decrease at least 61% and 48% for the bonded and sandwich reinforcement, respectively. According to Eurocode 3: Part 1-9 Fatigue[29], the fatigue strength curve of these welds is defined by the following equation (2):

$$\Delta\sigma = k \cdot n_f^{-1/3} \qquad (2)$$

$\Delta\sigma$ is the stress range, n_f is the fatigue life and k is a parameter which depends on the detail of the welds.

Taking into account the *SRF* close to the welds and rewriting equation (2), one can determine how much is the increase of the fatigue life of the welds after applying the reinforcement by equation (3):

$$\frac{\Delta\sigma^{reinf}}{\Delta\sigma^{Unreinf}} = \frac{k}{k} \cdot \left(\frac{n_f^{reinf}}{n_f^{Unreinf}} \right)^{-\frac{1}{s}} \Leftrightarrow n_f^{reinf} = \frac{n_f^{Unreinf}}{(1-SRF)^s} \tag{3}$$

Therefore, due to the reinforcement, the fatigue life of the deck-plate-to-stiffener welds at the crossbeam location is expected to increase at least 6 times (*SRF* = 45%) after applying the bonded steel plates reinforcement, and at least 4 times (*SRF* = 37%) after applying the sandwich steel plates reinforcement. At midspan between crossbeams, the fatigue life of the welds is expected to increase at least 15 times (*SRF* = 60%) after applying the bonded reinforcement and 7 times (*SRF* = 48%) after applying the sandwich reinforcement.

7. Conclusions

The aim of the research was to investigate the effect and the behaviour of the bonded and sandwich steel plates reinforcement systems when applied full scale orthotropic deck panels. The bonded steel plates system consisted of bonding a 6 mm thick second steel plate using a 2 mm thick adhesive layer. The sandwich steel plates system consisted of adding a 5 mm thick second steel plate using a 15 mm thick polyurethane core. Full-scale tests and FEA were performed on reinforced OBD to simulate heavy traffic wheel loads.

The results from the bonded steel plates reinforcement system showed a significant reduction of the transverse strains at the deck plate close to the deck-plate-to-stiffener welds. The strains at this deck location were reduced by at least 45% at the crossbeam and by at least 60% at midspan between crossbeams, after the reinforcement. This reduction is expected to increase 6 to 15 times the fatigue life of these welds after applying the bonded steel plates reinforcement.

The results from the sandwich steel plates reinforcement system also showed a significant reduction of the transverse strains at the deck plate close to the deck-plate-to-stiffener welds. The strains at this location were reduced by at least 40% at the crossbeam location and by at least 50% at midspan between crossbeams, after the reinforcement. This reduction is expected to increase 4 to 7 times the fatigue life of these welds after applying the sandwich steel plates reinforcement.

The suggested reinforcement systems showed a good performance and proved to be efficient lightweight solutions to refurbish orthotropic bridge decks and extend their life span.

Acknowledgements

The authors would like to thank Lightweight Structures B.V. and Intelligent Engineering (IE) for applying the reinforcements on the bridge deck specimens. This research was supported by the Dutch Technology Foundation STW (Project No. 05979) and by the Portuguese Science and Technology Foundation FCT (Grant No. SFRH/BD/36264/2007).

References

[1] Mangus A, Sun S. Orthotropic Deck Bridges. In W.-F. Chen and L. Duan (Eds.), Bridge engineering handbook, CRC Press, 2000; 1-47.

[2] Huang C, Mangus A, Copelan C. Icons of movable bridges utilizing orthotropic bridge decks. In 2010 Structures congress, Florida, USA, 2010; 3415–3430.

[3] Kolstein H, Wardenier J, Weijde H, A new type of fatigue failures in steel orthotropic bridge decks, In Fifth Pacific Structural Steel Conference, Seoul, Korea, 1998.

[4] Yuge T., Machida F, Morikawa H, Miki C, Kamiki T, Masui T. Analyses of fatigue damage patters in orthotropic steel deck of Tokyo metropolitan expressways. In 2004 Orthotropic Bridge Conference, Sacramento, California,USA, 2004.

[5] Wang C, Feng Y. Review of the fatigue behaviors and finite element analysis of orthotropic steel bridge decks. In International Orthotropic Bridge Conference 2008, Sacramento, California, USA, 2008.

[6] Pfeil MS, Battista RC, Mergulho AJ. Stress concentration in steel bridge orthotropic decks. Journal of Constructional Steel Research 2005; 61: 1172–1184.

[7] De Jong FBP, Renovation techniques for fatigue cracked orthotropic steel bridge decks, PhD thesis, Delft University of Technology, 2006.

[8] Xiao ZG. Yamada K, Ya S, Zhao XL. Stress analyses and fatigue evaluation of rib-to-deck joints in steel orthotropic decks. International Journal of Fatigue, 2008; 30: 1387–1397.

[9] Ya S, Yamada K, Ishikawa T. Fatigue evaluation of rib-to-deck welded joints of orthotropic steel bridge deck. Journal of Bridge Engineering 2011; 16 (4): 492–499.

[10] Miki C. Fatigue damage in orthotropic steel bridge decks and retrofit work. Steel structures 2006; 6: 255–267.

[11] Medani T, X. Liu X, Huurman M, Scarpas A, Molenaar A.. Experimental and numerical characterization of a membrane material for orthotropic steel deck bridges: Part 1: Experimental work and data interpretation. Finite Elements in Analysis and Design 2008; 44 (9-10): 552–563.

[12] Liu, X., T. Medani, A. Scarpas, M. Huurman, and A. Molenaar. Experimental and numerical characterization of a membrane material for orthotropic steel deck bridges: Part 2. Finite Elements in Analysis and Design 2008; 44 (9-10): 580–594.

[13] Walter R., Olesen JF, Stang H, Vejrum T. Analysis of an orthotropic deck stiffened with a cement-based overlay. Journal of Bridge Engineering 2007; 12 (3): 350–363.

[14] Murakoshi J, Yanadori N, Ui T, Inokuchi S, Ishigaki T, Kodama T, Oguri N. Research on steel fiber reinforced concrete pavement on orthotropic steel deck. In International Orthotropic Bridge Conference 2008, Sacramento, California, USA, 2008; 359–371.

[15] Labordus M. Vacuum infused bonded steel reinforcing plates for bridge rehabilitation. In International Bridge Technology Conference and Trade Show, Rotterdam, the Netherlands. Bridge Engineering, 2006.

[16] Vincent R, Ferro A. A new orthotropic bridge deck: Design, fabrication and construction of the shenley bridge incorporating a sps orthotropic bridge deck. In 2004 Orthotropic Bridge Conference, Sacramento, California, USA, 2004.

[17] Feldmann M, Sedlacek G, Geβler A. A system of steel-elastomer sandwich plates for strengthening orthotropic bridges decks. Mechanics of Composite Materials 2007; 43 (2): 183–190.

[18] Zhang D, Li Y, Cui C. A retrofitted case study of orthotropic steel bridge decks strengthened with sandwich plate system. Advanced Materials Research 2011; 163-167:410–416.

[19] Teixeira de Freitas S, Kolstein H, Bijlaard F. Composite bonded systems for renovations of orthotropic steel bridge decks, Composite Structures 2012; 92: 853–862.

[20] Teixeira de Freitas S, Kolstein H, Bijlaard F. Sandwich system for renovation of orthotropic steel bridge decks, Journal of Sandwich Structures and Materials 2011; 13 (3): 279–301.

[21] Teixeira de Freitas S, Kolstein H, Bijlaard F. Fatigue behavior of bonded and sandwich systems for strengthening orthotropic bridge decks, Composite Structures 2013; 97: 117–128.

[22] Teixeira de Freitas S, Kolstein H, Bijlaard F. Structural monitoring of a strengthened orthotropic steel bridge deck using strain data, Structural Health Monitoring 2012, 1 (5): 558–376.

[23] EN 1993-1-1. Eurocode 3: Design of steel structures Part1-1: General Rules and rules for buildings, 2006.

[24] ISO 8501. Preparation of steel substrates before application of paints and related products, 2007.

[25] EN 1991-2. Eurocode 1: Actions on structures – Part 2: Traffic loads on bridges, 2003.

[26] ABAQUS. Abaqus Version 6.8 Documentation. USA: Dassault Systèmes Simulia Corp., 2008.

[27] Teixeira de Freitas S, Steel plate reinforcement of orthotropic bridge decks, PhD Thesis, Delft University of Technology, 2012.

[28] Teixeira de Freitas S, Kolstein H, Bijlaard F. Parametric study on the interface layer of renovation solutions for orthotropic bridge decks, Computer-Aided Civil and Infrastructures Engineering 2012, 25(2): 143-153.

[29] EN 1993-1-9. Eurocode 3: Design of steel structures Part1-9: Fatigue, 2005.

.

Figure captions

Figure 1 –Typical cross section of an orthotropic steel bridge deck.

Figure 2 - Geometry of the orthotropic steel deck specimens (dimensions in mm).

Figure 2(a) Longitudinal view.

Figure 2(b) Transverse view.

Figure 3 – Reinforcement systems (dimensions in mm).

Figure 3 (a) Bonded steel plates.

Figure 3(b) Sandwich steel plates.

Figure 4 – Strain gauges at the midspan and crossbeam cross-sections (dimensions in mm).

Figure 4 (a) Midspan cross-section

Figure 4 (b) Top view of the midspan cross-section

Figure 4 (c) Crossbeam A cross-section

Figure 4 (d) Top view of the crossbeam cross-section

Figure 5 – Strain gauges close to the deck-to-stiffener weld.

Figure 6- Example of a static test performed at the crossbeam location (dimensions in mm).

Figure 6 (a) Longitudinal view

Figure 6 (b) Crossbeam A cross-section

Figure 7- Static test performed at midspan between crossbeam using wheel type B (dimensions in mm).

Figure 7 (a) Longitudinal view

Figure 7 (b) Midspan cross-section

Figure 8 – Test set-up overview.

Figure 9 - Three-dimensional finite element model overview.

Figure 10 - Mesh of the -FE model.

Figure 10 (a) top view of half of the deck plate.

Figure 10 (b) longitudinal view of the trough

Figure 10 (c) half of the crossbeam cross section.

Figure 10 (d) weld detail at the midpsan cross section

Figure 11 - Mesh details along the deck plate thickness (Y-axis).
Figure 11 (a) unreinforced deck
Figure 11 (b) bonded reinforced deck
Figure 11 (c) sandwich reinforced deck

Figure 12 – Transverse strains ε_{xx} at the crossbeam cross-section (CB) and 75 mm from the crossbeam (75 mm CB) on the bottom side of the deck plate recorded during testing (Exp) and predicted by the FEA (wheel type C at the crossbeam).
Figure 12 (a) bonded system
Figure 12 (b) sandwich system

Figure 13 – Transverse strains ε_{xx} at midspan between crossbeams on the bottom side of the deck plate recorded during testing (Exp) and predicted by the FEA (wheel load type C at midspan between crossbeams).
Figure 13 (a) bonded system: wheel type C at midspan.
Figure 13 (b) sandwich system: wheel type C at midspan

Figure 14 – Transverse strains ε_{xx} at midspan between crossbeams on the bottom side of the deck plate recorded during testing (Exp) and predicted by the FEA (wheel load type B at midspan between crossbeams).
Figure 14 (a) bonded system: wheel type B at midspan
Figure 14 (b) sandwich system: wheel type B at midspan.

Figure 15 – Transverse strains ε_{xx} at the bottom side of the deck plate given by the FEA (wheel type C, 100 kN).
Figure 15 (a) crossbeam cross-section
Figure 15 (b) midspan between crossbeams

Figure 16 – Groups of strain gauges.

Figures

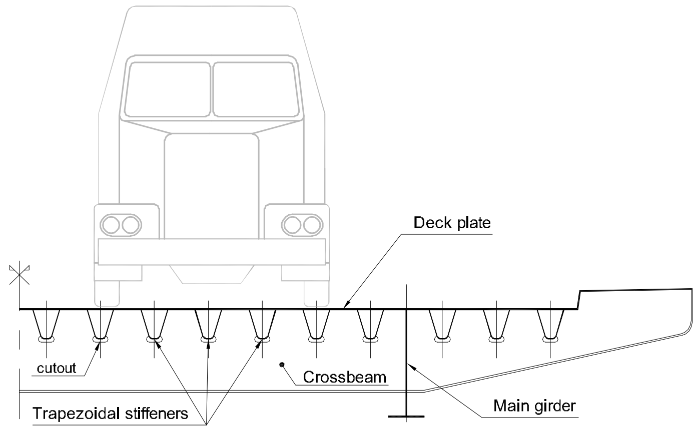

Figure 1: Typical cross section of an orthotropic steel bridge deck.

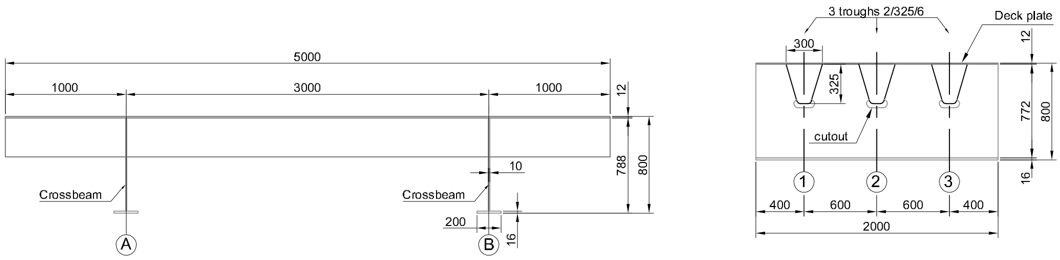

(a) Longitudinal view

(b) Transverse view

Figure 2: Geometry of the orthotropic steel deck specimens (dimensions in mm).

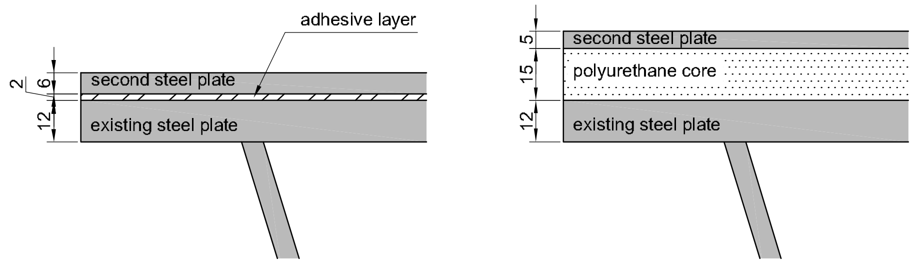

(a) Bonded steel plates

(b) Sandwich steel plates

Figure 3: Reinforcement systems (dimensions in mm).

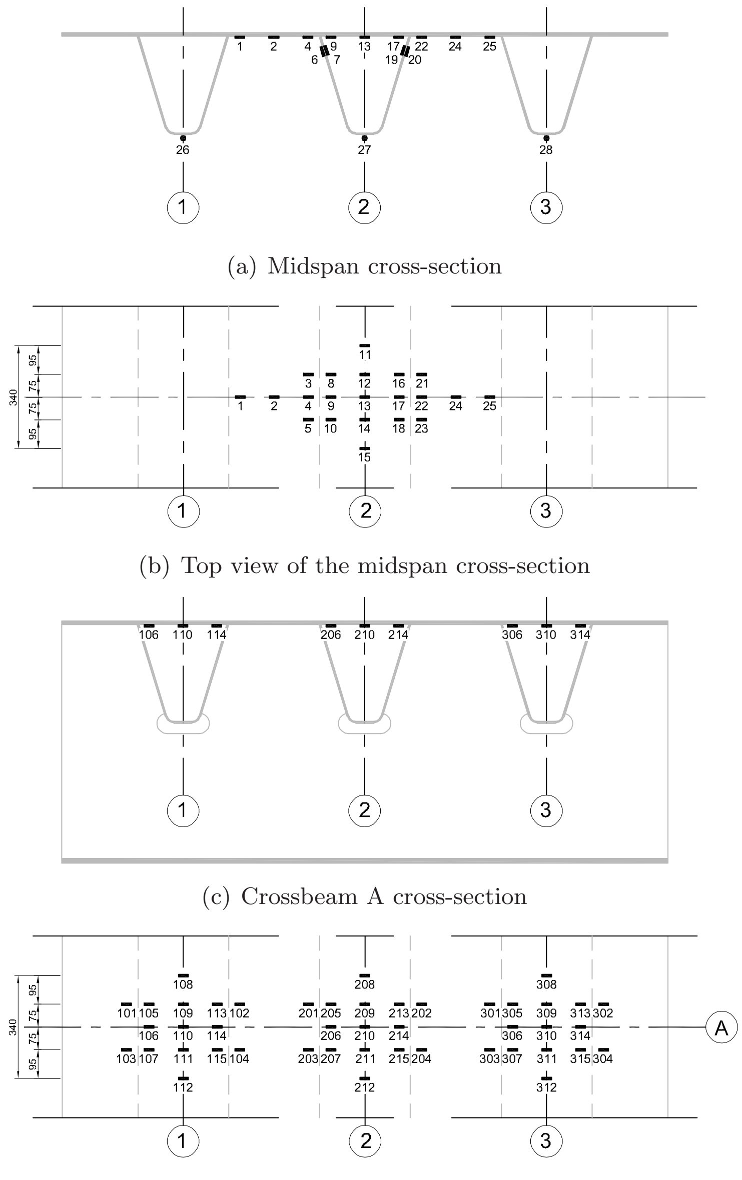

(a) Midspan cross-section

(b) Top view of the midspan cross-section

(c) Crossbeam A cross-section

(d) Top view of the crossbeam cross-section

Figure 4: Strain gauges at the midspan and crossbeam cross-sections (dimensions in mm).

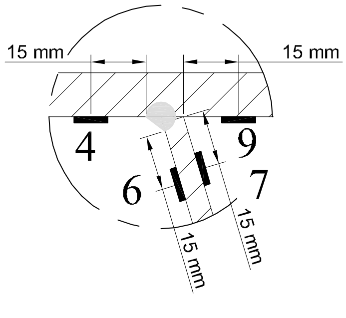

Figure 5: Strain gauges close to the deck-to-stiffener weld.

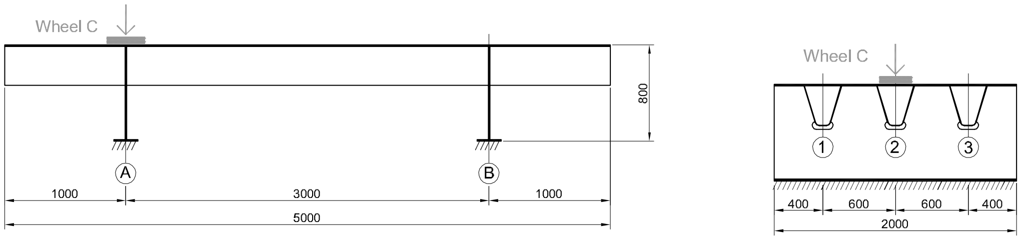

(a) Longitudinal view (b) Crossbeam A cross-section

Figure 6: Example of a static test performed at the crossbeam location (dimensions in mm).

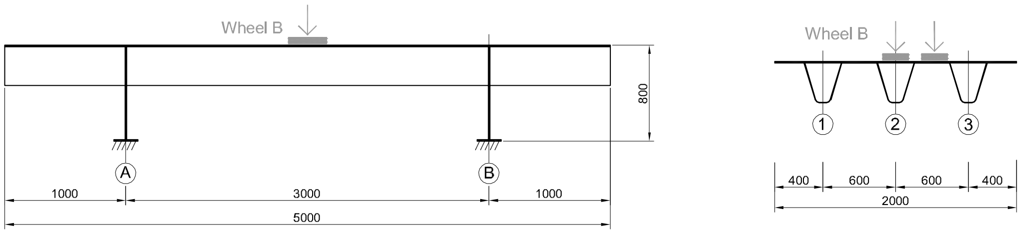

(a) Longitudinal view (b) Midspan cross-section

Figure 7: Static test performed at midspan between crossbeam using wheel type B (dimensions in mm).

Figure 8: Test set-up overview.

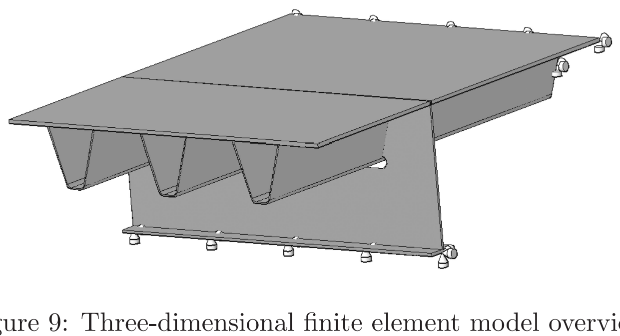

Figure 9: Three-dimensional finite element model overview.

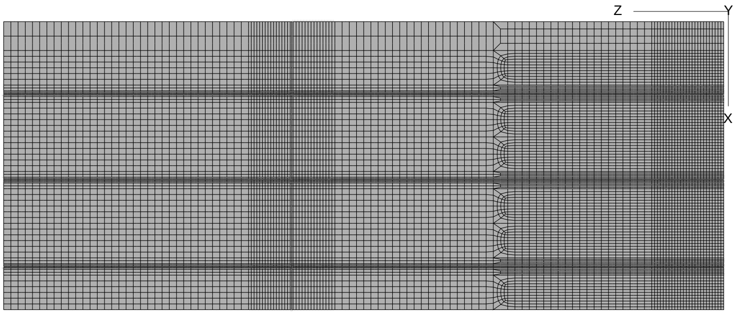

(a) top view of half of the deck plate

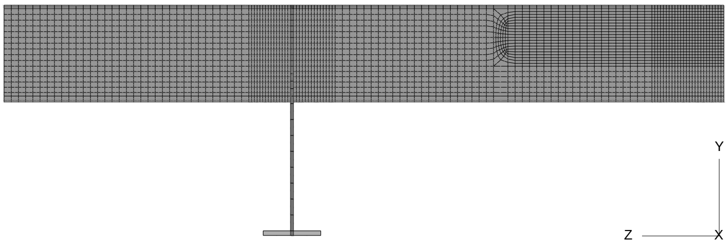

(b) longitudinal view of the trough

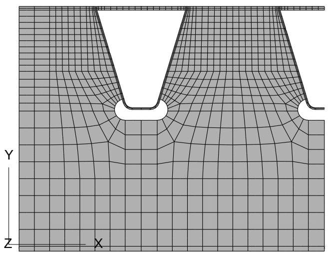

(c) half of the crossbeam cross section

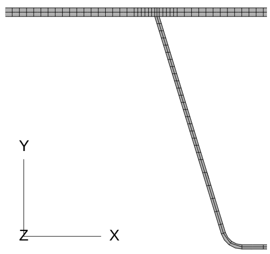

(d) weld detail at the midpsan cross section

Figure 10: Mesh of the FE-model.

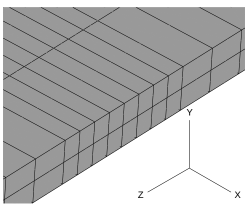

(a) unreinforced deck

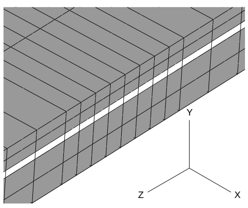

(b) bonded reinforced deck

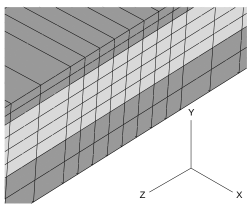

(c) sandwich reinforced deck

Figure 11: Mesh details along the deck plate thickness (Y-axis).

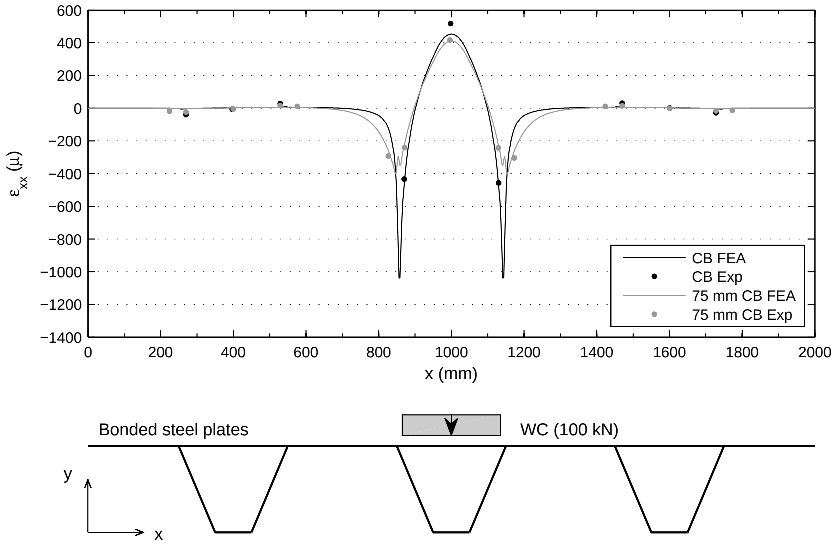

(a) bonded system

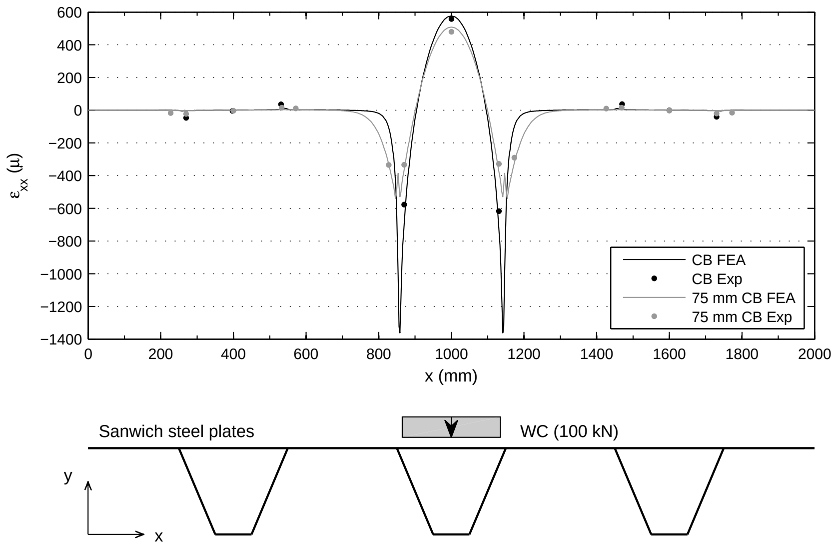

(b) sandwich system

Figure 12: Transverse strains ε_{xx} at the crossbeam cross-section (CB) and 75 mm from the crossbeam (75 mm CB) on the bottom side of the deck plate recorded during testing (Exp) and predicted by the FEA (wheel type C at the crossbeam).

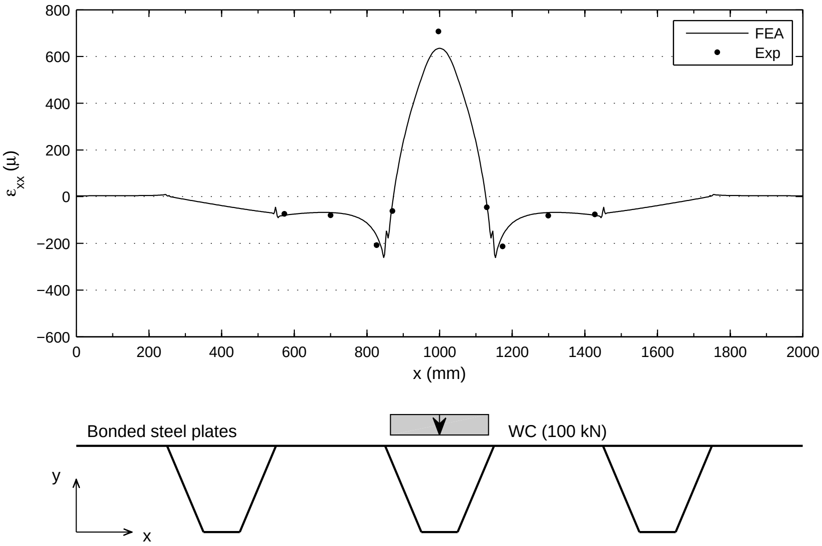

(a) bonded system: wheel type C at midspan

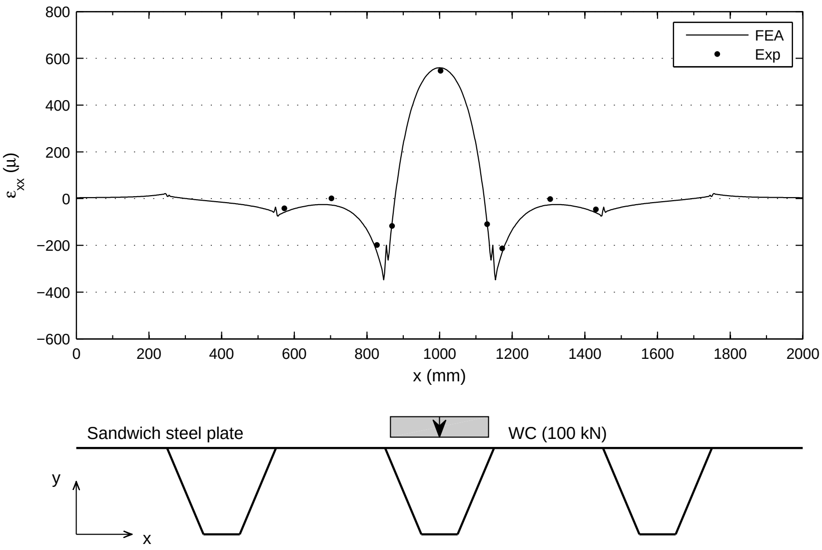

(b) sandwich system: wheel type C at midspan

Figure 13: Transverse strains ε_{xx} at midspan between crossbeams on the bottom side of the deck plate recorded during testing (Exp) and predicted by the FEA (wheel load type C at midspan between crossbeams).

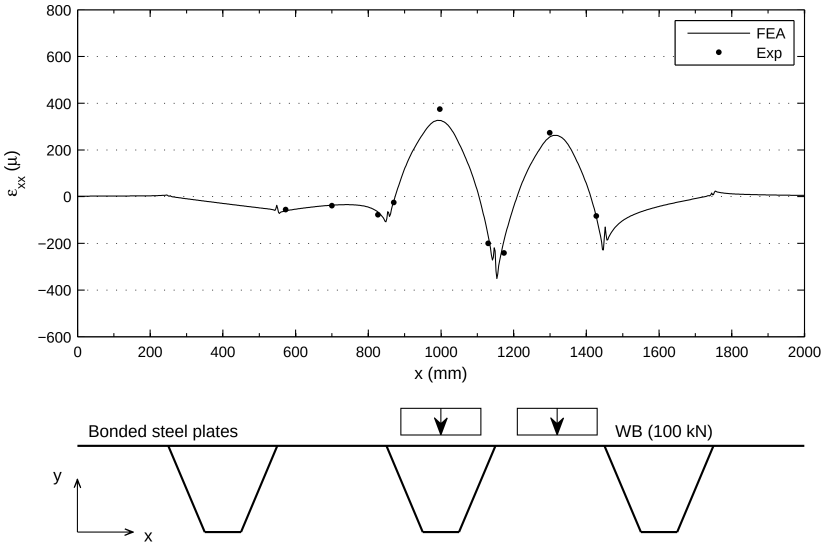

(a) bonded system: wheel type B at midspan

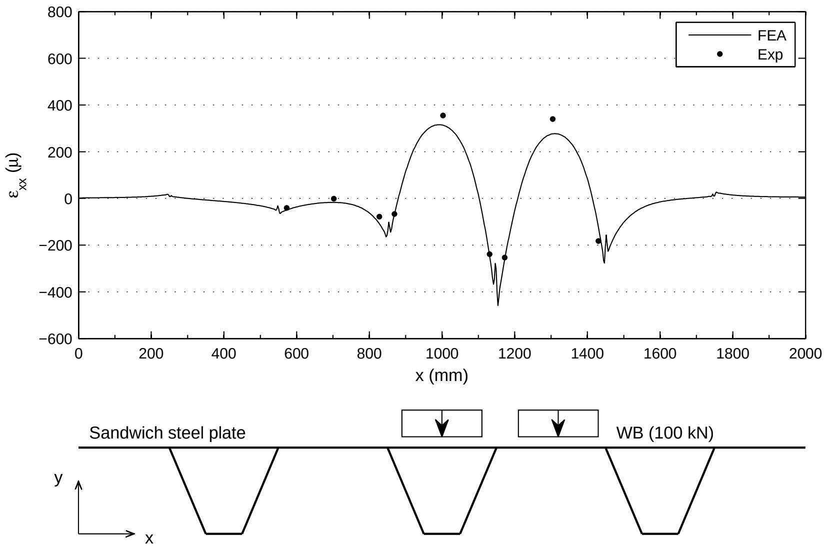

(b) sandwich system: wheel type B at midspan

Figure 14: Transverse strains ε_{xx} at midspan between crossbeams on the bottom side of the deck plate recorded during testing (Exp) and predicted by the FEA (wheel load type B at midspan between crossbeams).

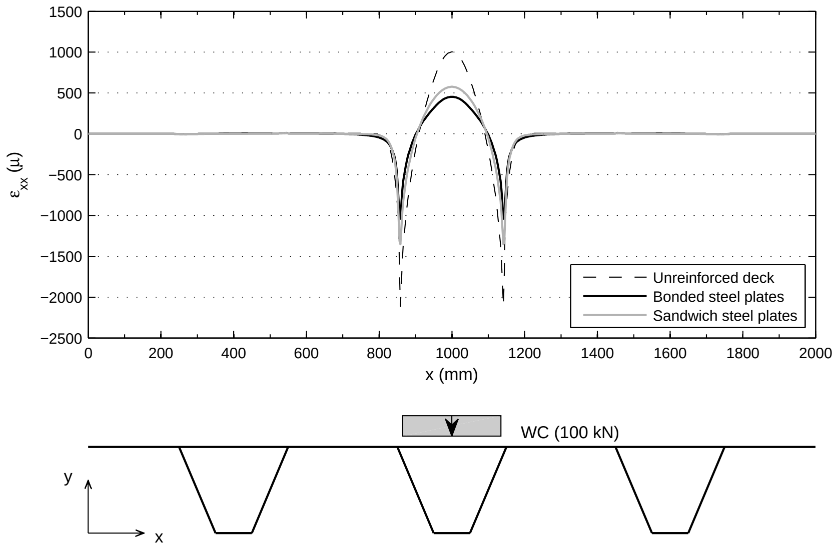

(a) crossbeam cross-section

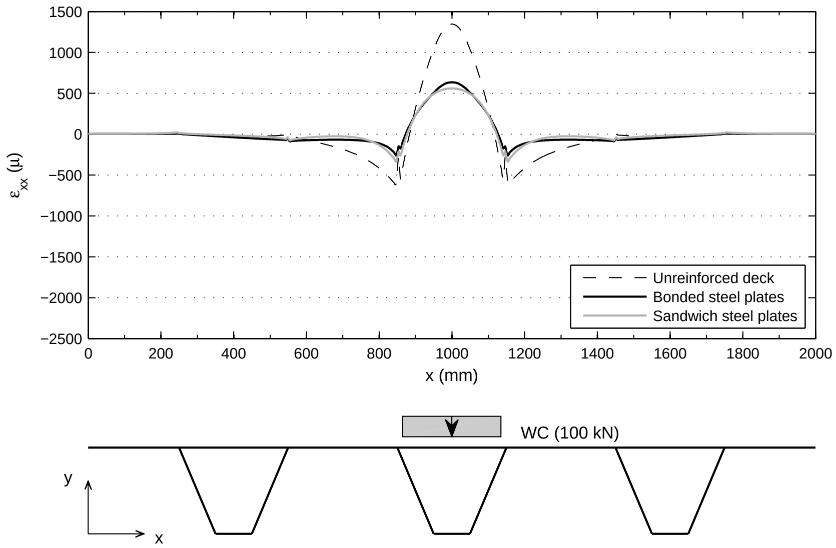

(b) midspan between crossbeams

Figure 15: Transverse strains ε_{xx} at the bottom side of the deck plate given by the FEA (wheel type C, 100 kN).

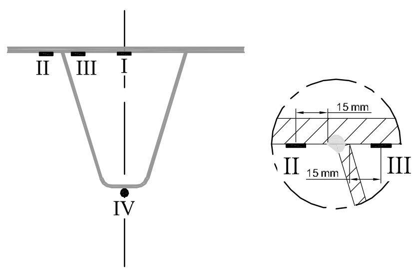

Figure 16: Groups of strain gauges.